

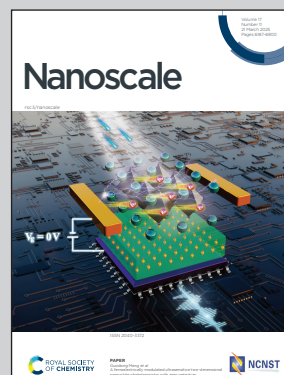
Showcasing research from Professor Pier Paolo Pompa's laboratory, NanobiInteractions&NanoDiagnostics, Istituto Italiano di Tecnologia (IIT), Italy.

Gold nanozymes for efficient degradation of organic dye pollutants: outperforming natural enzymes

This work provides insights into how Au-based nanozyme outperforms other nanozymes as well as natural peroxidase enzymes. It also introduces a proof-of-concept dye-degrading filter system, demonstrating its potential in real-world applications for environmental remediation.

Image reproduced by permission of Pier Paolo Pompa from *Nanoscale*, 2025, **17**, 6505.

As featured in:



See Pier Paolo Pompa *et al.*, *Nanoscale*, 2025, **17**, 6505.



Cite this: *Nanoscale*, 2025, **17**, 6505

Gold nanozymes for efficient degradation of organic dye pollutants: outperforming natural enzymes†

Giulia Mirra,^{‡a,b} Lorenzo Cursi,^{ID ‡a} Marina Veronesi,^{ID c} Luca Boselli^{ID a} and Pier Paolo Pompa^{ID *a}

Nanozymes (NZs) are raising increasing interest as effective tools for the degradation of organic pollutants dispersed in the environment. In particular, noble-metal NZs are extremely efficient and versatile, thanks to their multi-enzymatic activities, wide pH operational range, and thermal stability. However, whilst multifunctionality can be a key asset of NZs in some applications (e.g., by intrinsic self-cascade/tandem reactions), the “internal” competition between their different catalytic activities may strongly limit their specific efficiency towards some targets. In this scenario, a deep comprehension of their catalytic mechanisms and careful optimization of the operating conditions are crucial to disclose their full potential and maximize their performances. Here, we analyzed the ability of gold, palladium, and platinum NZs to degrade model organic pollutants of industrial relevance, *i.e.* rhodamine B, methylene blue, and methyl orange. Interestingly, we found that AuNZ is very efficient in degrading all three dyes *via* peroxidase-like activity, unlike the natural enzyme (horseradish peroxidase – HRP), which displayed weak degradative capabilities. On the other hand, Pd and PtNZs experience the internal competitive catalase-like reaction, strongly limiting their dye degradation performances. The mechanism underlying AuNZ’s ability to degrade the synthetic dyes was investigated, revealing the preferential reactivity with the aromatic structures of the molecules. We also developed a proof-of-concept AuNZ-based dye-degrading filter system, showing excellent dye removal capability and good recyclability, even in real environmental samples.

Received 6th December 2024,

Accepted 3rd February 2025

DOI: 10.1039/d4nr05137h

rsc.li/nanoscale

Introduction

Synthetic dyes are widely employed in several industrial sectors, such as textile, painting, printing, pharmaceuticals, cosmetics, and paper.^{1,2} However, they represent a serious threat when released in the environment, especially into water bodies: even at trace level, they can perturb light penetration, adversely affecting aquatic photosynthesis and consequently lowering oxygen availability for aquatic species.^{1,2} Furthermore, they are often classified as toxic or carcinogenic, both for humans and aquatic fauna.^{1,3} Notably, the complex aromatic and conjugated groups in their molecular structure,

responsible for their characteristic color, are typically resistant to biodegradation, thus they persist for long times in the environment.^{4,5}

The treatment of synthetic dye contaminated waters mainly relies on “non-destructive” methods (adsorption, coagulation/flocculation, and filtration methods) that transfer the color from liquid to solid waste.^{3,4,6,7} However, these methods can hardly be considered a solution, since the solid waste can still represent a hazard for the environment and requires careful disposal. Advanced oxidizing processes⁸ such as photocatalysis and electrocatalysis are emerging as possible alternatives. These new technologies allow for mineralization of organic dyes,^{9–11} yet they are often energetically expensive, due to the necessity of power supply to produce UV light and current.¹²

Nanozymes (NZs), nanomaterials that mimic the activity of natural enzymes,^{13,14} have recently been proposed as an alternative tool for synthetic dye degradation.^{12,15–18} NZs offer wider pH and temperature operational range^{19,20} and are, in general, more robust than their natural counterparts,^{21,22} making them appealing in the field of pollutant remediation. Some drawbacks, however, include incomplete comprehension of their multifunctional catalytic behavior along with lack of

^aNanobiointeractions&Nanodiagnostics, Istituto Italiano di Tecnologia (IIT), Via Morego 30, Genova 16163, Italy. E-mail: pierpaolo.pompa@iit.it

^bDepartment of Chemistry and Industrial Chemistry, University of Genova, Via Dodecaneso 31, Genova 16146, Italy

^cStructural Biophysics Facility, Istituto Italiano di Tecnologia (IIT), Via Morego 30, Genova 16163, Italy

† Electronic supplementary information (ESI) available. See DOI: <https://doi.org/10.1039/d4nr05137h>

‡ Equally contributing authors.



substrate selectivity, which often limit their applicability. On the other hand, one NZ might potentially remove a plethora of contaminants. Au, Pd, and PtNZs are emerging nanotools that present multi-enzymatic activity,^{22–24} being able to mimic oxidase- (OX-), peroxidase- (POD-) and catalase-like (CAT-like) activities simultaneously, and they are therefore extremely versatile systems.

As previously reported, these NZs can catalytically oxidize a substrate (such as an organic dye) *via* OX-like or POD-like activity, thus using O₂ or H₂O₂ as co-substrates, respectively. Alternatively, *via* CAT-like reaction, these NZs can lead to the disproportionation of H₂O₂. POD- and CAT-like activities are thus in competition. In both cases, the first step of the process is the NZ reaction with H₂O₂ forming highly reactive transient species (HRI*) at the surface (including hydroxyl radicals).^{21,24,25} During the second step, these reactive intermediates can, in one case, mainly react among them, or with another molecule of H₂O₂, eventually forming O₂ and H₂O, or instead react with a different substrate, such as a chromogenic one, oxidizing it. The highly oxidative reactions involved in the POD-like activity of NZs can also lead to multiple oxidations and eventually to oxidative degradation of a substrate,^{3,26} especially because, unlike their natural counterparts, NZs could exploit a remarkably high H₂O₂ concentration to boost the peroxidation processes.²¹ Furthermore, the possibility of immobilizing NZs on various supports facilitates their practical reuse, thus enhancing the relative economic feasibility.^{15,16,27}

In this work we investigated the performances of Au, Pd, and PtNZs in the degradation of three widely employed synthetic dyes, *i.e.* Rhodamine B (RhB), Methylene Blue (MB), and Methyl Orange (MO). While other studies have started to explore the potential of NZs in this context,^{28–30} this work deepens the processes behind the degradation efficiency of different noble-metal NZs for specific organic dyes, analyzing their mechanisms and the differences with the activity of a natural peroxidase. We found that the multifunctionality and intrinsic competitive reactions of NZs are crucial to define their overall catalytic performance. Notably, the high CAT-like activity of Pt and PdNZs was found to strongly interfere with the process of dye degradation *via* POD-like activity. In contrast, despite AuNZs typically exhibit lower POD-like activity compared to Pt and PdNZs,²⁴ they demonstrated superior efficiency in organic dye degradation, thanks to the lower interference of competitive CAT-like reaction. Interestingly, the degradation efficiency and versatility achieved by the AuNZ largely outperformed the activity of the natural horse radish peroxidase (HRP) enzyme, which was quite ineffective against the synthetic dyes analyzed herein.

Results and discussion

Au, Pd, and PtNZs are among the most promising NZs in several fields, thanks to their high catalytic efficiency and multiple enzyme-like activities.^{21,31} They have shown impressive POD-like activity²¹ that could be exploited in many

applications,^{32–35} including environmental pollution remediation.^{36,37}

To best compare their performance in this field, we synthesized and characterized Au, Pd, and PtNZs with similar size (about 4 nm) and used citrate as capping agent to normalize their surface chemistry. The NZs were characterized by TEM and DLS, showing monodisperse and colloidal stable aqueous suspensions (Fig. S1–3†).

We chose RhB as our first target since it is one of the most employed synthetic dyes in industry, it is difficult to biodegrade, and it has been reported to be hazardous and carcinogenic.⁶ The reaction conditions (NZ and H₂O₂ concentrations) for RhB degradation *via* POD-like activity were optimized for each NZ (Fig. S4†). AuNZs resulted the most effective (Fig. 1A): a dispersion of 44 nM can degrade >90% of a concentrated RhB solution (40 μM) in the presence of H₂O₂.

In contrast, despite similar size and surface chemistry, Pd and PtNZs degraded only about 10% of RhB primarily within the first 10 minutes, after which their activity ceased. Notably, in the reaction solution of Pd and PtNZs, we observed intense and rapid bubble formation (oxygen development), while no bubbles were detectable in the reaction containing AuNZs. Monitoring the O₂ production with a sensor in the same reaction conditions (Fig. 1B), we confirmed that oxygen was quickly and intensively produced in the presence of Pd and PtNZs, while almost no oxygen development was detected in the presence of AuNZs. These results clearly indicate that, in these experimental conditions, the strong competitive CAT-like activity rapidly consumed the H₂O₂ substrate necessary for POD functionality, thus completely inhibiting the POD-mediated degradation of RhB dye by Pd and PtNZs after a few minutes.

This outcome was not specific to RhB degradation. We tested the performance of the NZs against other two organic dyes commonly used in industrial applications, namely MB and MO (Fig. S5†). Similarly, AuNZ turned out to be very effective in the degradation of both dyes (Fig. 1C and D). In the case of MO, the difference in the degradation performance between Au and Pt/Pd was striking. With MB dye, Pt and Pd showed some POD-like activity at early time points (similar to Au), however after 10 min their degradation functionality underwent strong inhibition. Interestingly, the POD-mediated degradations of both MB and MO were consistent with the competitive CAT mechanism mentioned above: Pd and PtNZs were not able to degrade these synthetic dyes because they consumed most of the H₂O₂ *via* CAT-like side reaction (Fig. S6†). Indeed, replenishing the H₂O₂ in the reaction solutions with a fresh aliquot, the degradation of the dyes resumed (Fig. S7†). Overall, this suggests that multifunctionality and internal competitive activities of nanozymes can be crucial in the design and development of applications targeting specific substrates.

Considering the superior performance exhibited by AuNZs with all the dyes tested, we focused on this functional material to get a deeper insight into the degradation mechanism, further optimize its performance, and make a direct compari-



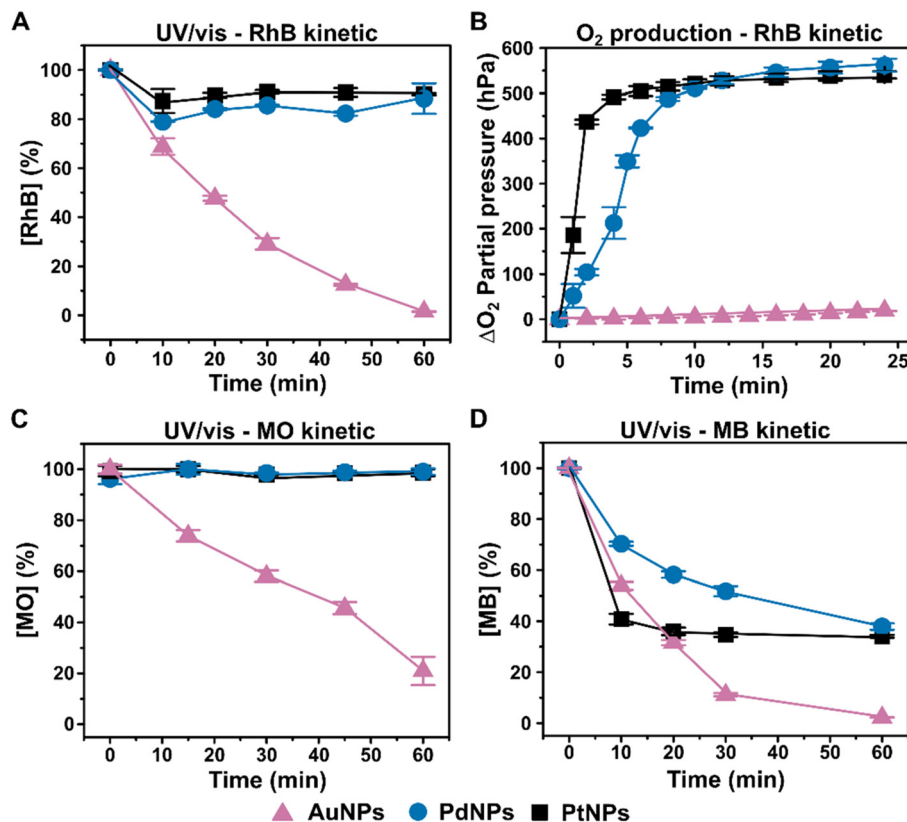


Fig. 1 Performance of Au, Pd, and PtNZs in degrading different organic dyes. (A) Kinetic of RhB degradation using Au, Pd, and PtNZs, 40 μM dye and 0.4 M H_2O_2 . (B) CAT-like activity of the different NZs in the same conditions of (A). (C) Kinetics of MO degradation and (D) MB degradation using Au, Pd, and PtNZs, 40 μM dye and 0.4 M H_2O_2 . In each experiment, the NZ concentration was normalized to have the same total surface area. Data are plotted as average \pm standard deviation of three replicates.

son against a natural peroxidase enzyme (HRP), which can be used as a reference tool in this kind of environmental remediation applications.^{38–41} Since it is well established that the physical–chemical environment can significantly affect the activity of NZs,²¹ as a first point we investigated the performance of AuNZs in different pH, temperatures, and buffers. We observed that the process of dyes degradation *via* POD-like activity of AuNZs is favored under basic conditions (average 40% activity increase with all the 3 dyes with respect to neutral pH, see Fig. 2A), also due to the better colloidal stability of this nanomaterial in alkaline environment (Fig. S8[†]). Noteworthy, the performance of AuNZs is strongly enhanced (up to 8–9 times) by increasing the temperature from 20 to 70 °C, depending on the dye (Fig. 2B). This enhancement is attributed to the higher POD-like activity of AuNZ rather than to thermal degradation of the dye in these conditions (Fig. S9[†]). Such catalytic features are important in view of practical applications, since at the optimal pH and temperature it may be possible to achieve very efficient and fast degradation of the synthetic dyes, unlike biological enzymes that are typically unfolded/degraded at mid-high temperatures.²¹ In this respect, we analyzed the behavior of the natural enzyme (HRP), for direct comparison with the AuNZ in the degradation of the 3 synthetic dyes. Importantly, HRP was able to catalyze some

degradative effects on MO, but was completely ineffective with the other two dyes, likely due to the lack of recognition of RhB and MB as enzymatic substrates. This was observed in very different conditions of H_2O_2 concentration (1–400 mM range); indeed, at the highest concentration, the natural HRP quickly lost its efficiency even with the MO dye (Fig. 2C), because of the harsh conditions, unlike the artificial AuNZ, which therefore exhibited unique performances in terms of versatility and efficiency.

MO solution treated with HRP was not completely decolorized after treatment, probably due to the formation of some colored byproducts, as suggested by the UV-vis spectra (Fig. S10[†]). Indeed, as analyzed in more detail in the following, the HRP enzyme did not elicit full degradation also in the case of MO, displaying rather a partial oxidation/decoloration of the dye.^{42–44}

We also tested the activity of AuNZs in the presence of different buffers (Fig. S11[†]). The NZs were fairly stable in the presence of all the buffers, except TRIS (Fig. S12[†]), but their activity decreased significantly when TRIS, carbonate, or borate buffers were used. On the contrary, we observed no interference from HEPES buffer, which was thus selected as the buffer of choice for the following experiments mimicking real applications (see below).



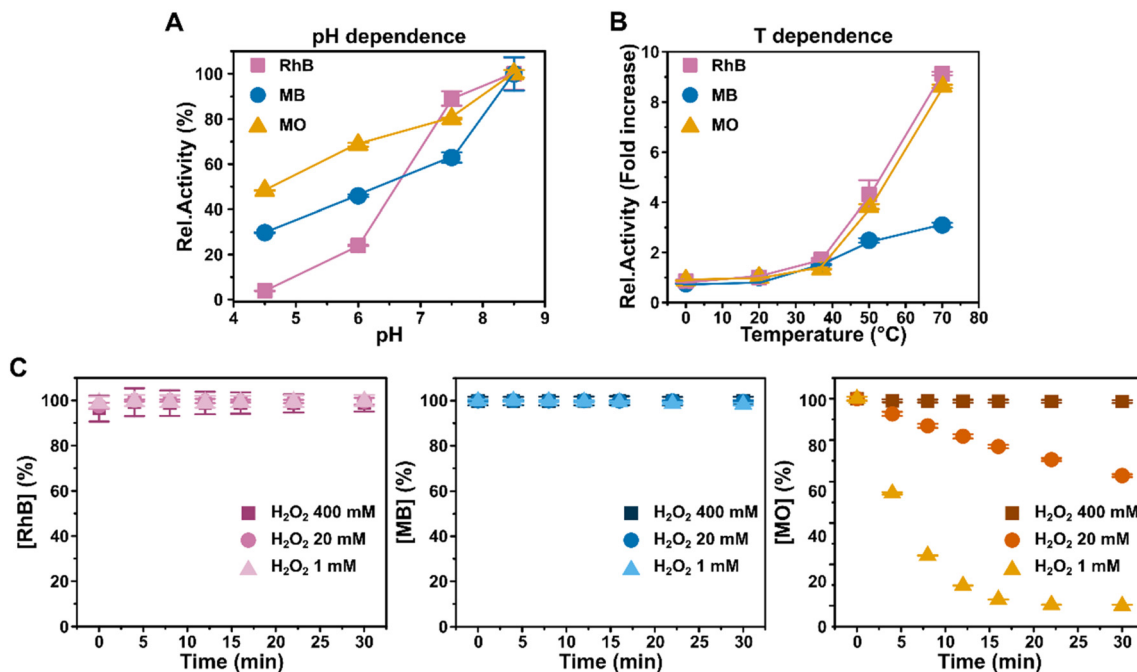


Fig. 2 Effect of pH and temperature on AuNZ performance and comparison with natural HRP enzyme. Degradation of the three dyes by AuNZs as a function of (A) pH and (B) temperature. Data were normalized to the maximum activity obtained with each dye. (C) Natural horseradish peroxidase (20 ppm) shows no activity with RhB (10 μ M) and MB (14 μ M), while it can oxidize MO (40 μ M), when used with low H₂O₂ concentrations.

We tried to investigate the mechanism underlying the AuNZ ability to degrade the synthetic dyes. First, we observed that, when the 3 dyes are simultaneously present in the solution, they are all degraded, though with different efficiency: first MB, then RhB, and MO (Fig. 3). To understand this pattern, we calculated the apparent Michaelis-Menten constants (K_m) for the reaction with the different dyes and H₂O₂ (Fig. S13 and S14[†]).

The apparent K_m represents the affinity of a substrate for the enzyme: the lower the K_m the higher the affinity.⁴⁵ Our

results show that the sequence of dye degradation follows the order of the apparent K_m , starting from MB ($K_m = 12 \mu$ M) then RhB ($K_m = 40 \mu$ M) and finally MO ($K_m = 90 \mu$ M). Thus, the dyes are degraded in succession, from the one with the highest affinity to the one with the lowest, in an almost selective way.

As a further characterization step, we analyzed the AuNZ-based degradation process of the organic dyes by NMR. It has been reported that dye degradation catalyzed by Fenton-like reactions can lead to complete oxidation of the organic molecules to H₂O and CO₂.^{4,16,27} We thus analyzed our dye solu-

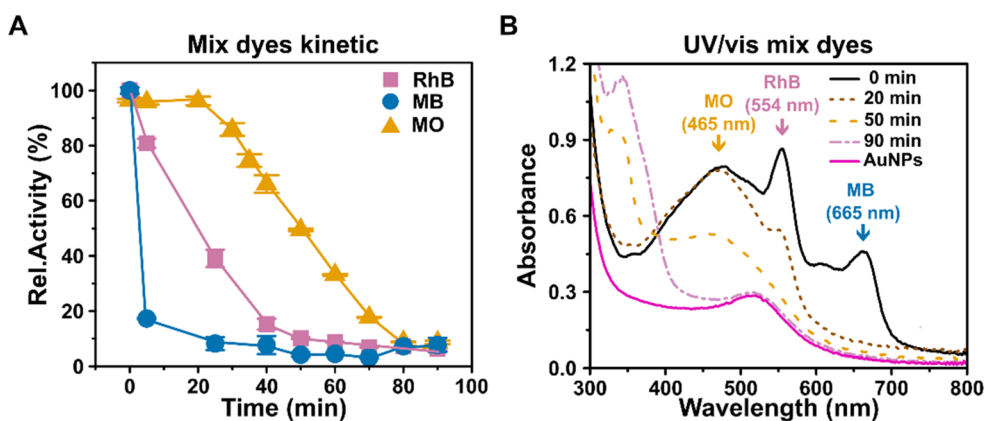


Fig. 3 Au NZ degrading mixed dye solution. (A) Degradation of a mix containing 10 μ M RhB, 14 μ M MB, and 40 μ M MO with AuNZs. Data are plotted as average \pm st. deviation of three replicates. (B) UV-vis spectra of the mixed dye solution during the degradation with AuNZs at different time points (the peaks at 465, 554, and 665 nm are the characteristic absorption peaks of MO, RhB, and MB, respectively). Three consecutive aliquots of H₂O₂ were added at interval of 20 minutes in order to completely decolorize the solution.



tions before and after the AuNZ treatment in the presence of increasing concentration of H_2O_2 (Fig. 4A, B and S15–17†). For all the dyes, the NMR spectra show that the signals of aromatic protons (~ 7.0 – 8.0 ppm range) disappear with increasing H_2O_2 concentrations, while new signals appear in the aliphatic region (below 4.0 ppm). This suggests that the AuNZs degrade the aromatic system of the synthetic dyes, most likely *via* Fenton-like reaction (as already reported for other NZs),^{16,25,27} possibly leading to complete mineralization of the organic molecules. On the contrary, when treating MO with HRP

(Fig. 4C and S16B†), the signals of aromatic protons do not disappear completely, although they decrease in intensity and shift. Accordingly, the MO solution does not appear completely clear upon HRP treatment, unlike the one treated by AuNZ (Fig. 4C, right). This confirms that, in these conditions, HRP is not capable of mineralizing the synthetic dye, but it only oxidizes the molecule, probably forming different byproducts. However, due to the complexity of the NMR spectra in the aliphatic region, further investigations are necessary beyond NMR to clearly identify the various degradation products.

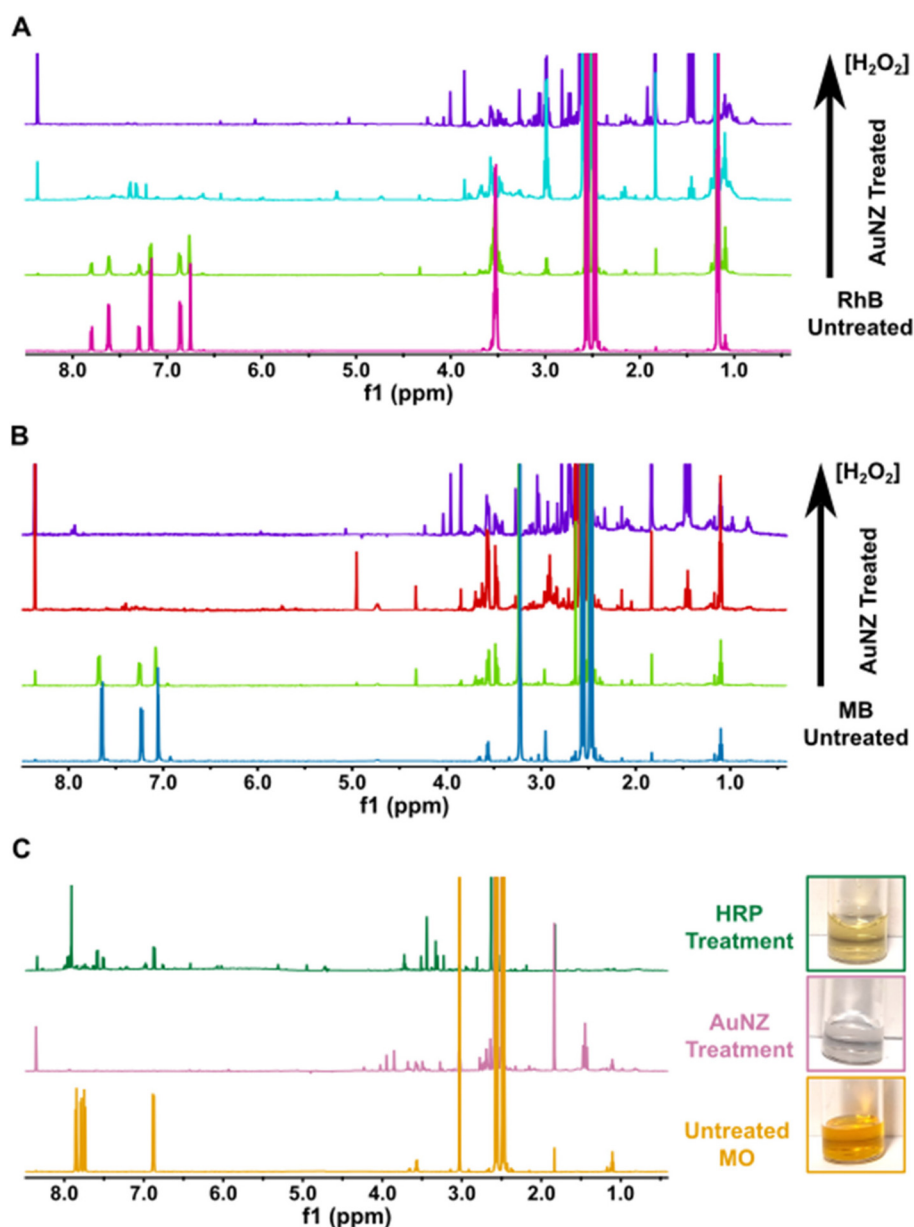


Fig. 4 Comparison among ^1H 1D NMR spectra of the dye degradation products. (A) $100\ \mu\text{M}$ RhB solution before and after the treatment with $15\ \text{ppm}$ AuNZ with increasing concentrations of H_2O_2 (10 , 100 , and $1000\ \text{mM}$ from bottom to top). (B) $100\ \mu\text{M}$ MB solution before and after the treatment with $15\ \text{ppm}$ AuNZ with increasing concentrations of H_2O_2 (10 , 100 , and $1000\ \text{mM}$ from bottom to top). (C) Comparison of the final MO solutions before and after treatment with $20\ \text{ppm}$ HRP and $5\ \text{mM}$ H_2O_2 or $15\ \text{ppm}$ AuNZ and $500\ \text{mM}$ H_2O_2 . The photos show the difference in color intensity between the untreated solution and those treated with AuNZ or HRP. All the ^1H 1D NMR spectra and pictures were acquired after $24\ \text{h}$ of treatment to guarantee all the H_2O_2 was consumed.



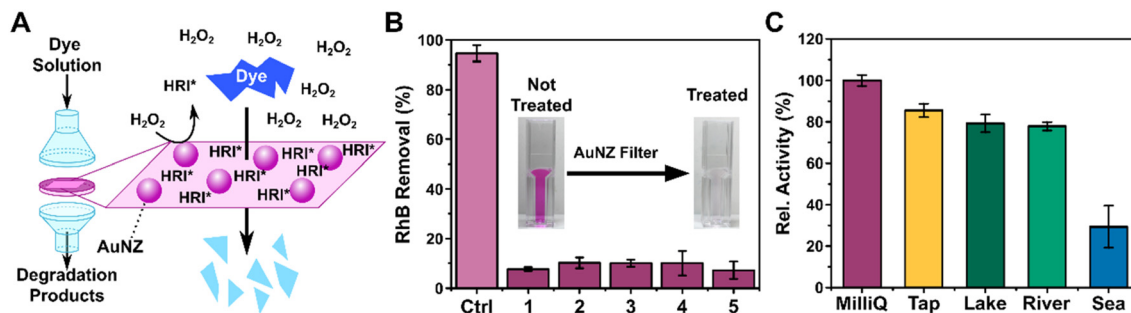


Fig. 5 Proof-of-concept system for dyes degradation by AuNZs in real-world scenario. (A) Schematic of the proof-of-concept system: the dye solution is pushed through the AuNZ filter, the highly reactive intermediates (HRI*), formed at the AuNZ surface from the H_2O_2 in the reaction solution, promote the dye degradation; the treated solution is then collected and analyzed. (B) Performance of the system for the degradation of RhB ($10\ \mu\text{M}$) over repeated filtration cycles of 5 different samples. (C) Performance of the system with RhB-spiked ($10\ \mu\text{M}$) real samples: comparison of the degradation efficiency in milliQ water *versus* tap, lake, river, and sea water. Data are plotted as average \pm standard deviation of three replicates.

These results suggest that the AuNZ could be effective also on other emerging pollutants, in particular those with large aromatic groups, including some antibiotics as well as chemotherapeutic and anti-inflammatory drugs.

We finally designed a proof-of-concept filtering system to prove the suitability of the nanozymes to degrade the synthetic dyes in simulated real-world applications. The immobilization of the AuNZs onto a membrane provides an easy and effective way for their integration in a continuous flow system that simplifies both the reuse and the scale-up of the remediation process (Fig. 5A and Fig. S18[†]). Moreover, it also enables NZ stabilization and optimal activity even in complex media, *e.g.* at high ionic strength. As reported in Fig. 5B, using 1 mL solution of RhB ($10\ \mu\text{M}$) in presence of H_2O_2 , we observed >90% degradation of the dye by the AuNZs. In these conditions, the optimal degradation process required 3 filtrations steps, due to the short contact time between the sample and the NZs/membrane system (Fig. S19[†]) (see Methods for details). In view of future on-field applications, the presented “device” could be implemented by using filter chains (or immobilizing the NZ on columns) and/or inserting it in a continuous flow circulating system. Notably, this model system worked properly in terms of recyclability: the same AuNZ-based filter was tested with multiple cycles of dye degradation, and we observed no detectable loss of efficiency after 5 full RhB degradations (Fig. 5B). This is interesting as it confirms the high stability of the NZs together with their tolerance to harsh conditions (see also Fig. 2).

Finally, we tested the performance of the device with real samples. We prepared spiked solutions of RhB using tap, lake, river, and sea water and we compared the degradation performance of the AuNZ-filter *versus* pure laboratory water (milliQ). The results showed that tap, lake, and river waters do not cause strong interferences with the catalytic performance of the device (Fig. 5C). In the case of sea water, we observed a drop of efficiency with *ca.* 30% performance; however, the device proved its degradation capability even in such high ionic strength medium and using an unrealistically high dye concentration.

Conclusions

In this work, we explored the behavior of three noble-metal NZs, namely Au, Pd, and PtNZs, for the catalytic degradation of different synthetic dyes of industrial relevance. Our results highlight that a deep understanding of the NZs multi-enzymatic activity is essential to properly exploit their features. Indeed, AuNZ resulted the most efficient, despite showing lower POD-like activity, thanks to a negligible competitive interference from its CAT-like activity. On the contrary, Pt and PdNZs preferentially consumed H_2O_2 substrate *via* CAT-like activity, showing minor POD-like degradation activity towards the synthetic dyes. Interestingly, the natural HRP enzyme was found to be mostly ineffective against the organic pollutants. We also investigated the process of dye degradation by NMR, observing a preferential activity on the aromatic structure of the molecules. The reaction conditions were optimized to maximize the performance of the AuNZ, and a proof-of-concept dye-degrading filter system was implemented allowing for recovery and reuse of the nanocatalyst. The system showed excellent performance, being able to degrade more than 90% of the dye in contaminated solutions and excellent robustness with simulated real samples (contaminated tap, river, lake, and sea waters). These results may contribute to disclosing the potential of nanozymes for environmental remediation and sustainability applications and may encourage future studies with other classes of pollutants and multifunctional systems.

Data availability

The data that support the findings of this study are available from the corresponding author, upon reasonable request.

Conflicts of interest

There are no conflicts to declare.



Acknowledgements

This work is part of the “Technologies for Sustainability” Flagship program of the Italian Institute of Technology (IIT).

References

- 1 A. Tkaczyk, K. Mitrowska and A. Posylniak, *Sci. Total Environ.*, 2020, **717**, 137222.
- 2 A. K. D. Alsukaibi, *Processes*, 2022, **10**, 1968.
- 3 C. Zaharia and D. Suteu, in *Organic Pollutants Ten Years After the Stockholm Convention*, ed. P. Tomasz and M.-S. Aleksandra, IntechOpen, Rijeka, 2012, ch. 3, DOI: DOI: [10.5772/32373](https://doi.org/10.5772/32373).
- 4 M. C. Collivignarelli, A. Abbà, M. Carnevale Miino and S. Damiani, *J. Environ. Manage.*, 2019, **236**, 727–745.
- 5 S. M. Ghoreishi and R. Haghghi, *Chem. Eng. J.*, 2003, **95**, 163–169.
- 6 A. V. Mohod, M. Momotko, N. S. Shah, M. Marchel, M. Imran, L. Kong and G. Boczkaj, *Water Resour. Ind.*, 2023, **30**, 100220.
- 7 F. McYotto, Q. Wei, D. K. Macharia, M. Huang, C. Shen and C. W. K. Chow, *Chem. Eng. J.*, 2021, **405**, 126674.
- 8 J. Mukherjee, B. K. Lodh, R. Sharma, N. Mahata, M. P. Shah, S. Mandal, S. Ghanta and B. Bhunia, *Chemosphere*, 2023, **345**, 140473.
- 9 F. Costantino, A. Armirotti, R. Carzino, L. Gavioli, A. Athanassiou and D. Fragouli, *J. Photochem. Photobiol., A*, 2020, **398**, 112599.
- 10 A. Houas, H. Lachheb, M. Ksibi, E. Elaloui, C. Guillard and J.-M. Herrmann, *Appl. Catal., B*, 2001, **31**, 145–157.
- 11 A. A. Özcan and A. Özcan, *Chemosphere*, 2018, **202**, 618–625.
- 12 Q. Feng, G. Wang, L. Xue, Y. Wang, M. Liu, J. Liu, S. Zhang and W. Hu, *ACS Appl. Nano Mater.*, 2023, **6**, 4844–4853.
- 13 J. Wu, X. Wang, Q. Wang, Z. Lou, S. Li, Y. Zhu, L. Qin and H. Wei, *Chem. Soc. Rev.*, 2019, **48**, 1004–1076.
- 14 M. Liang and X. Yan, *Acc. Chem. Res.*, 2019, **52**, 2190–2200.
- 15 R. Dadigala, R. Bandi, M. Alle, C.-W. Park, S.-Y. Han, G.-J. Kwon and S.-H. Lee, *J. Hazard. Mater.*, 2022, **436**, 129165.
- 16 L. Wang, L. Zhao, D. Si, Z. Li, H. An, H. Ye, Q. Xin, H. Li and Y. Zhang, *Sep. Purif. Technol.*, 2024, **331**, 125571.
- 17 M. J. Jacinto, R. S. Souto, V. C. P. Silva, I. C. Prescilio, A. C. Kauffmann, M. A. Soares, J. R. de Souza, A. F. Bakuzis and L. C. Fontana, *Water, Air, Soil Pollut.*, 2021, **232**, 270.
- 18 Q. Diao, X. Chen, Z. Tang, S. Li, Q. Tian, Z. Bu, H. Liu, J. Liu and X. Niu, *Environ. Sci.:Nano*, 2024, **11**, 766–796.
- 19 A. Shamsabadi, T. Haghghi, S. Carvalho, L. C. Frenette and M. M. Stevens, *Adv. Mater.*, 2024, **36**, 2300184.
- 20 L. Gao, H. Wei, S. Dong and X. Yan, *Adv. Mater.*, 2024, **36**, 2305249.
- 21 L. Cursi, G. Mirra, L. Boselli and P. P. Pompa, *Adv. Funct. Mater.*, 2024, **34**, 2315587.
- 22 J. Sheng, Y. Wu, H. Ding, K. Feng, Y. Shen, Y. Zhang and N. Gu, *Adv. Mater.*, 2024, **36**, 2211210.
- 23 M. Zandieh and J. Liu, *Adv. Mater.*, 2024, **36**, 2211041.
- 24 G. Mirra, L. Cursi, L. Boselli and P. P. Pompa, *Small Sci.*, 2024, 2400487.
- 25 N. Li, R. Li, Z. Li and X. Liu, *New J. Chem.*, 2024, **48**, 11407–11419.
- 26 Y. Deng and R. Zhao, *Curr. Pollut. Rep.*, 2015, **1**, 167–176.
- 27 T. Yang, X. Liu, Z. Zeng, X. Wang, P. Zhang, B. Feng, K. Tian and T. Qing, *Environ. Pollut.*, 2023, **316**, 120643.
- 28 Z. Gao, H. Wu, Z. Liu, L. Liu, Z. Zeng, X. Yang, H. Wang, J. Du, B. Zheng and Y. Guo, *ACS Appl. Nano Mater.*, 2023, **6**, 11531–11540.
- 29 X. Zhao, T. Yang, D. Wang, N. Zhang, H. Yang, X. Jing, R. Niu, Z. Yang, Y. Xie and L. Meng, *Anal. Chem.*, 2022, **94**, 4484–4494.
- 30 Q. Li, D. Yu, C. Fan, Q. Huang, Y. Tang, R. Guo, Y. Huang, H. Wang, C. Lin and Y. Lin, *ACS Appl. Nano Mater.*, 2022, **5**, 94–100.
- 31 Y. Ai, Z.-N. Hu, X. Liang, H.-B. Sun, H. Xin and Q. Liang, *Adv. Funct. Mater.*, 2022, **32**, 2110432.
- 32 E. De Luca, D. Pedone, A. Scarsi, R. Marotta, F. Catalano, D. Debellis, L. Cursi, B. Grimaldi, M. Moglianetti and P. P. Pompa, *Small Sci.*, 2024, **4**, 2400085.
- 33 G. Tarricone, V. Castagnola, V. Mastronardi, L. Cursi, D. Debellis, D. Z. Ciobanu, A. Armirotti, F. Benfenati, L. Boselli and P. P. Pompa, *Nano Lett.*, 2023, **23**, 4660–4668.
- 34 A. Scarsi, D. Pedone and P. P. Pompa, *Nanoscale Adv.*, 2023, **5**, 2167–2174.
- 35 T. Pomili, P. Donati and P. P. Pompa, *Biosensors*, 2021, **11**, 2777–2809.
- 36 G. Fang, R. Kang, S. Cai and C. Ge, *Nano Today*, 2023, **48**, 101755.
- 37 Y. Meng, W. Li, X. Pan and G. M. Gadd, *Environ. Sci.:Nano*, 2020, **7**, 1305–1318.
- 38 N. Elmerhi, K. Al-Maqdi, K. Athamneh, A. K. Mohammed, T. Skorjanc, F. Gándara, J. Raya, S. Pascal, O. Siri, A. Trabolsi, I. Shah, D. Shetty and S. S. Ashraf, *J. Hazard. Mater.*, 2023, **459**, 132261.
- 39 M. Bilal, H. M. N. Iqbal, H. Hu, W. Wang and X. Zhang, *J. Environ. Manage.*, 2017, **188**, 137–143.
- 40 S. M. A. Guelli Ulson de Souza, E. Forgiarini and A. A. Ulson de Souza, *J. Hazard. Mater.*, 2007, **147**, 1073–1078.
- 41 S. V. Mohan, K. K. Prasad, N. C. Rao and P. N. Sarma, *Chemosphere*, 2005, **58**, 1097–1105.
- 42 T. S. Shaffiqu, J. J. Roy, R. A. Nair and T. E. Abraham, *Appl. Biochem. Biotechnol.*, 2002, **102**, 315–326.
- 43 M. Ambatkar and U. Mukundan, *Appl. Water Sci.*, 2015, **5**, 397–406.
- 44 V. S. Ferreira-Leitão, J. G. da Silva and E. P. S. Bon, *Appl. Catal., B*, 2003, **42**, 213–221.
- 45 P. K. Robinson, *Essays Biochem.*, 2015, **59**, 1–41.

